

# A Preliminary Study of Andrographolide Precipitation from *Andrographis Paniculata* Extracts Using a Supercritical Anti-Solvent (SAS)

**Photchanathip Imsanguan, Suwassa Pongamphai,  
Supaporn Douglas and Wittaya Teppaitoon**

Department of Chemical Engineering, Faculty of Engineering,  
King Mongkut's University of Technology Thonburi, Bangkok 10140, Thailand  
E-mail: suwassa.pon@kmutt.ac.th

**Peter L. Douglas**

Department of Chemical Engineering, University of Waterloo, Ontario, Canada N2L 3G1

## Abstract

The aim of this research was to study the effect of pressure (5-24 MPa) and temperature (308-328 K) on the precipitation of andrographolide from *Andrographis paniculata* extracts. Andrographolide was precipitated using ethanol and compressed CO<sub>2</sub> as the so-called anti-solvent at a constant CO<sub>2</sub> flow rate of 1 g/min. The efficiency of two precipitation methods; Supercritical Anti-Solvent (SAS) process and evaporation process were compared. For the SAS process, the crystal particles were obtained as *column-like* and *slice-like* depending on the operating conditions. The mean diameters were found to be in the range of 5.36–34.01 µm. Small particles with narrow size distributions were obtained at the high pressure and low temperature. Moreover, high performance liquid chromatography (HPLC) also indicated that the SAS process demonstrated a high yield and high degree of purity. On the other hand, the precipitates obtained from subcritical anti-solvent and evaporation process were amorphous particles and high impurities. The SAS process was found to be the successful precipitation method for andrographolide precipitation from *A. paniculata* extracts because of uniform crystal, small particle size, narrow size distribution, high precipitation yield and selective precipitation.

**Keywords:** Andrographolide; *Andrographis paniculata*; Precipitation; Supercritical anti-solvent

## 1. Introduction

Micronization, particle shape and size distribution of drug are necessary for controlling drug release such as decreasing the required dosage of drug, increasing the bioavailability of drug in the body [1]. The conventional micronization technique of the

pharmaceutical industry has some drawbacks such as large size distribution, high temperature, impurities in final product and environmental pollution. In recent years, micronization process using Supercritical Anti-Solvent (SAS) has been widely used in several segments such as pharmaceuticals,

food, polymer, catalyst materials, pigment powder, surface coating, and superconductor precursors [2, 3, 4, 5]. The SAS process can be used to modify the morphology, crystalline structure, size, and size distribution of particles, through the control of operating parameters such as pressure, temperature, flow rate, critical concentration of solution and solvent type, and can produce pure products with no residue solvent [6, 7].

In the SAS process, solute is dissolved in a liquid organic solvent, and then precipitated by addition of a supercritical anti-solvent that has a low affinity for the solute and a high affinity for the organic solvent. This method of particle formation is based on two mechanisms that take place simultaneously; the supercritical fluid penetrates into the droplets and organic solvent evaporates on supercritical fluid. Fast supersaturation is generated by both mass transfer processes so that the precipitation results in micro or nano particles [8, 9].

Andrographolide is the main substance in leaves of *A.paniculata*. It has been reported to have excellent anti-inflammatory, anti-bacterial, anti-viral effects [10], anti-platelet aggregation, hepatoprotective [5], anti-cancer activity against human leukemia HL-60 cells and other cancer cells [5, 11], help against fever, sore throat, and be a new way for treating HIV [12]. The chemical structure of andrographolide is shown in Fig. 1.

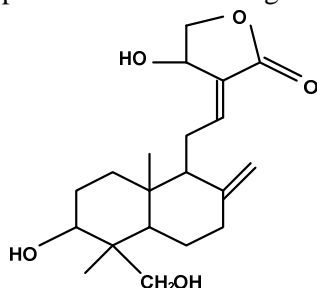


**Fig.1** The chemical structure of andrographolide

The aim of this research was to evaluate the influence of pressure and temperature on particle characteristics (morphology, crystalline structure, size and size distribution), and to compare the precipitation efficiency of supercritical anti-solvent and evaporation processes.

## 2. Experimental

### 2.1 Preparing solution

*A.paniculata* powder was extracted with ethanol in a volume ratio of 1 : 2 at a rotating speed of 200 rpm and temperature of 308 K for 2 h. The initial concentration of andrographolide in the extract was analyzed using High Performance Liquid Chromatography (HPLC). Andrographolide in the extracts was precipitated by both Supercritical Anti-Solvent (SAS) process and evaporation process as described below.

### 2.2 Andrographolide precipitation using SAS process

The SAS apparatus is shown in Fig. 2. The bottom of the crystallization vessel was equipped with a filter for collecting the precipitates. At the beginning of the experiment, the CO<sub>2</sub> was compressed by hydraulic pump before being induced into the crystallization vessel. The CO<sub>2</sub> was allowed to flow through the system for 15 min for steady state. Next, the *A.paniculata* extract was sprayed co-currently with CO<sub>2</sub> through the capillary nozzle for 2 h 30 min. Valve 4 was then closed and pure CO<sub>2</sub> was allowed to flow through the system to remove the solvent and dry precipitated particles for 4 h. The particles were collected and analyzed. The operating conditions were pressure range of 5–24 MPa, temperature range of 308–328 K and constant CO<sub>2</sub> flow rate and solution flow rate of 1 g/min and 0.13 mL/min, respectively.

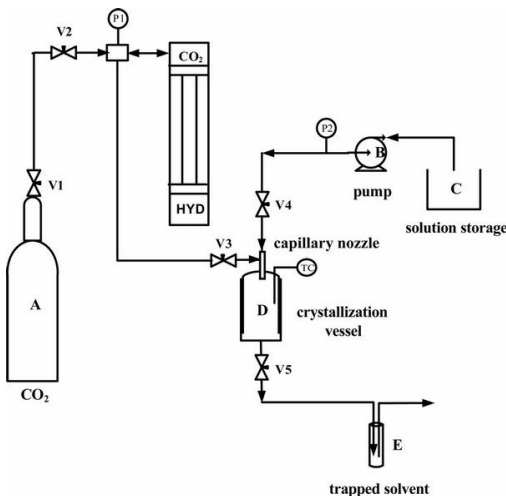


**Fig.2** A Schematic diagram of supercritical anti-solvent apparatus. (A)  $\text{CO}_2$  cylinder, (B) booster pump, (C) solution storage, (D) crystallization vessel, (E) trapped solvent or liquid effluent, (HYD) hydraulic pump, (V1, V2, V4, V5) needle valve, (V3) ball valve, (P1, P2) pressure gauge, (TC) temperature control.

### 2.3 Andrographolide precipitation using evaporation process

A 200 mL *A.paniculata* extract was heated at a constant temperature of 353 K for 2 h. The precipitates were analyzed to determine the particle characteristics.

### 2.4 Particle analysis

The morphology of precipitates was analyzed using a Scanning Electron Microscope (SEM) model LEO, 1455VP. The mean particle size and size distribution were measured with Image-Pro Plus software. The particles were analyzed with an X-ray diffraction (XRD), model BRUKER, D8DISCOVER to determine the effect of SAS process parameters on the crystalline structure. The crystal of andrographolide can be observed from the peaks at  $2\theta = 10^\circ$ ,  $12^\circ$ ,  $15^\circ$  and  $16^\circ$  [5].

## 3. Results and Discussions

The initial concentration of andrographolide in *A.paniculata* extract was found to be 3.007 g/L. It is enough for

precipitating using SAS process. In this research, the effects of temperature and pressure on particle size, size distribution and morphology of particles were studied. An overview of the results is given in Table 1.

**Table 1** Summary of experimental performed

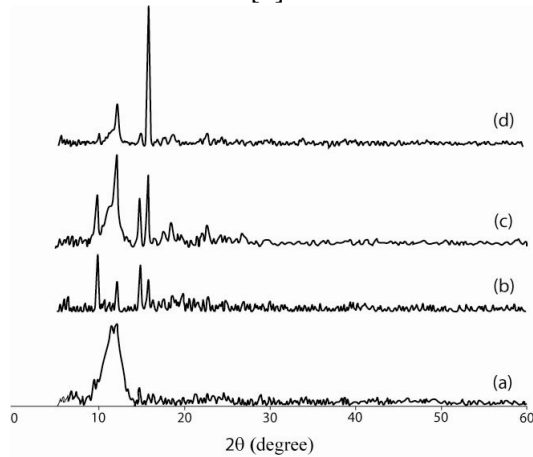
Run	P (MPa)	T (K)	Morphology	Mean particle size ( $\mu\text{m}$ )
1	5	308	amorphous	1.05
2	10	308	slice-like	10.51
3	10	318	slice-like	33.33
4	10	328	amorphous	6.67
5	17	308	slice-like	8.23
6	24	308	column-like	5.36
7	evaporation		amorphous	110.44

### 3.1 Effect of pressure

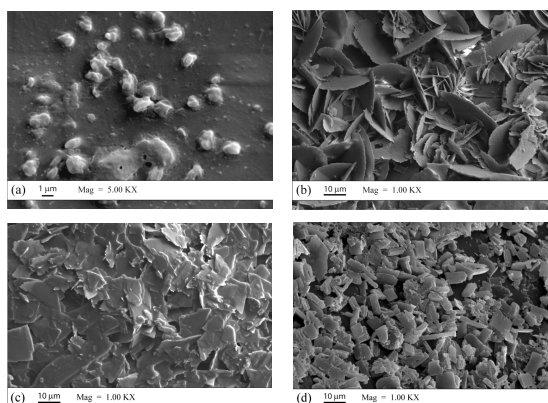
Precipitation using SAS process was carried out at a constant temperature of 308 K,  $\text{CO}_2$  flow rate of 1 g/min and a pressure varying from 5 to 24 MPa. Fig. 3 shows that the particles obtained at 5 MPa were amorphous particles, because the XRD pattern shows a broad peak. On the other hand, the particles obtained at 10-24 MPa were andrographolide crystal, because their four peaks of XRD patterns are sharp and match with the XRD pattern of andrographolide.

Fig. 4 shows SEM micrographs of the precipitated particles. These results confirm the results from XRD patterns that the particles obtained at 5 MPa seem not to have a fixed shape or amorphous particles as can be seen in Fig. 4a. Operation was under subcritical conditions, which was lean in  $\text{CO}_2$ , so ethanol was not completely miscible with  $\text{CO}_2$  leading to amorphous particle formation [13]. Whereas, andrographolide crystals which were *slice-like* and *column-like* were obtained at pressures of 10-17 and 24 MPa respectively, as can be seen in Fig. 4b-4d. The pressure range of 10 to 24 MPa with temperature of 308 K produced a supercritical condition. The  $\text{CO}_2$  completely miscible with ethanol led to

high supersaturation, fast nucleation rate and crystal growth rate resulting in crystal particle formation. Moreover, the influence of pressure also resulted in a difference of morphology, but the change of morphology did not relate with polymorphs, because *column-like* and *slice-like* exhibited similar XRD patterns as can be seen in Fig. 3b-3d. Therefore the change of morphology depends on the relative growth of a specific face, for example, *column-like* has an elongated growth in the vertical direction whereas *slice-like* has a growth in the horizontal direction [9].



**Fig.3** XRD patterns of andrographolide in the precipitated particles under SAS process at constant temperature of 308 K and various pressures; (a) 5 MPa; (b) 10 MPa; (c) 17 MPa and (d) 24 MPa.



**Fig.4** The SEM micrographs of the precipitated particles at constant temperature of 308 K and various pressures; (a) 5

MPa; (b) 10 MPa; (c) 17 MPa and (d) 24 MPa.

The mean particle size under supercritical condition decreased with increasing pressure, being 10.51  $\mu\text{m}$  at 10 MPa, 8.23  $\mu\text{m}$  at 17 MPa and 5.36  $\mu\text{m}$  at 24 MPa. The narrower size distribution obtained at the higher pressure can be seen in Fig. 5. The main effect of changing the operating pressure was to change the density of the supercritical  $\text{CO}_2$ . At high pressure, the  $\text{CO}_2$  density was higher; hence the solubility of  $\text{CO}_2$  in the ethanol also increased resulting in the short average lifetime of a droplet, high mass transfer rate, high supersaturation, fast nucleation rates and fast crystal growth rate. These then led to smaller particle size and narrower size distribution [14].

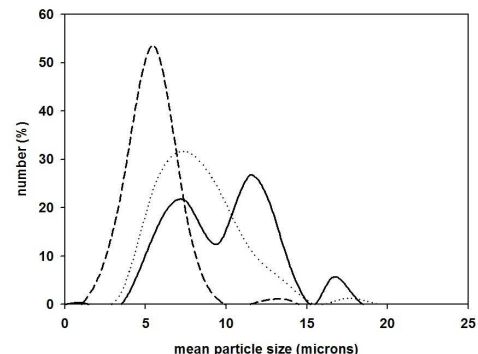


**Fig.5** The size distribution of the precipitated particles under SAS process at constant temperature of 308 K and various pressures; (—) 10 MPa; (.....) 17 MPa and (---) 24 MPa.

### 3.2 Effect of temperature

The effect of temperature on the precipitation was studied at constant pressure of 10 MPa, using  $\text{CO}_2$  flow rate of 1 g/min, and a temperature varying from 308 to 328 K. Fig. 6 shows that the particles obtained at 308 K and 318 K were andrographolide crystal. Whereas, the particles obtained at 328 K were amorphous particles because the XRD pattern shows a broad peak.

*Slice-like* particles were obtained at temperatures of 308 K and 318 K, while amorphous particles were obtained at 328 K as can be seen in Fig. 7a-7c. 10 MPa, 308 K and 10 MPa, 318 K are at supercritical conditions which have enough  $\text{CO}_2$  in droplets for dissolving ethanol, so  $\text{CO}_2$  is completely miscible with ethanol. This caused high supersaturation, fast nucleation rate, fast crystal growth rate leading to crystal formation. On the other hand, the particles obtained at 10 MPa, 328 K were amorphous particles since the operating point was below subcritical condition. Therefore, only a small amount of  $\text{CO}_2$  dissolved in ethanol leading to low supersaturation and amorphous particle formation.

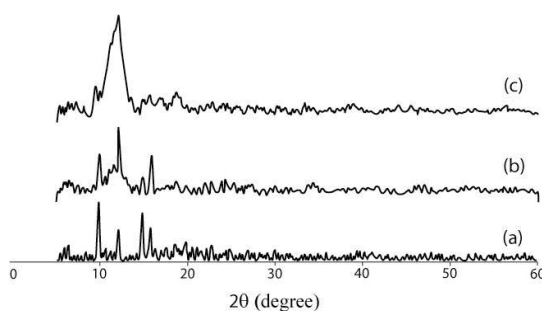


**Fig.6** XRD patterns of andrographolide in the precipitated particles under SAS process at constant pressure of 10 MPa and various temperatures; (a) 308 K; (b) 318 K and (c) 328 K.

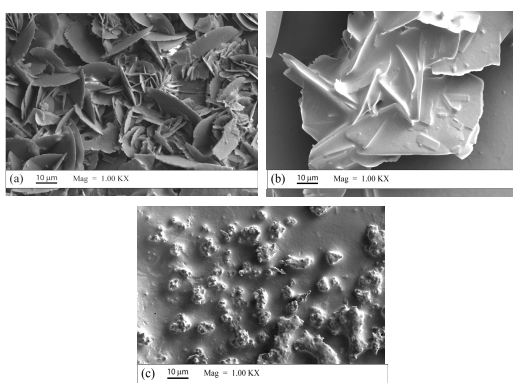


**Fig.7** The SEM micrographs of the precipitated particles at constant pressure of 10

MPa and various temperatures; (a) 308 K; (b) 318 K and (c) 328 K.

The mean particle size increased with increasing temperature under supercritical condition, being  $10.51 \mu\text{m}$  at 10 MPa, 308 K and  $33.33 \mu\text{m}$  at 10 MPa, 318 K. Moreover, a narrower size distribution was obtained at the lower temperature as can be seen in Fig. 8. When the temperature increases, the solubility of andrographolide in the ethanol increases. Therefore, the supersaturation is attained slower. As a result, the particle size increases [15].

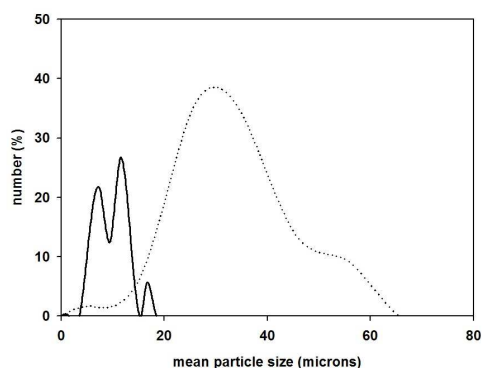


**Fig.8** The size distribution of the precipitated particles under SAS process at constant pressure of 10 MPa and various temperatures; (—) 308 K and (....) 318 K.

### 3.3 Comparison between SAS and evaporation processes

Fig. 9 shows the precipitated particles obtained in the evaporation process and its XRD pattern. The results show that the particles obtained in the evaporation process were amorphous particles. Moreover the XRD pattern of evaporated particles also show crystal structure of potassium compounds ( $2\theta = 28^\circ$ ,  $40^\circ$  and  $50^\circ$ ) but the XRD patterns of SAS precipitated particles have none. Therefore the SAS process is selective precipitation. SAS is more suitable than evaporation process because it can produce small crystal

particles, narrow size distribution and can control particle size, size distribution and crystal structure by controlling operating conditions whereas evaporation process can not.

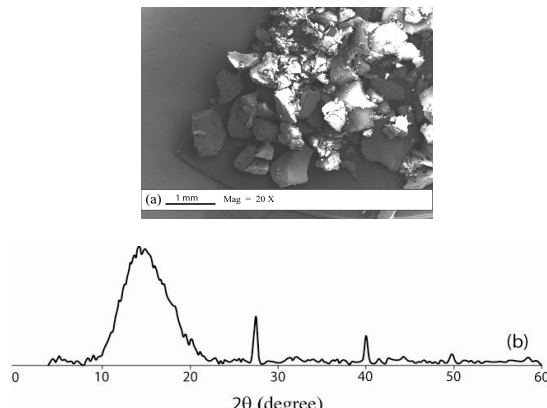


**Fig.9** (a) The SEM micrographs of the precipitated particles and (b) XRD pattern of andrographolide in the precipitated particles from the evaporation process at 353 K.

#### 4. Conclusion

The results indicated that the precipitation of andrographolide from *A.paniculata* extract was successfully performed using SAS process. The SAS process can produce uniform crystals of andrographolide, small particle size and narrow size distribution. The precipitation pressure and temperature were the most important variables that affected the precipitation process. The particle size decreased with increasing pressure in the range of 10–24 MPa and decreasing temperature in the range of 308–318 K under SAS process. On the other hand, the subcritical anti-solvent process (5 MPa, 308 K and 10 MPa 328 K) and evaporation process led to amorphous andrographolide particle formation.

Based on a comparison of the two precipitation methods (SAS process and evaporation process) it was concluded that the SAS process is more suitable for andrographolide precipitation from *A.paniculata* extract.

Precipitation using the SAS process results in crystal particles, small particle size, narrow size distribution, high purity, and selective precipitation.

#### 5. Acknowledgement

The authors gratefully acknowledge the financial support from the Thailand Research Fund (TRF) through the Royal Golden Jubilee Ph.D. Program (1.C.KT/47/G.1).

#### 6. References

- [1] Kikic I., Alessi P., Evaia F., Moneghini, M. and Perissutti B., Supercritical Antisolvent Precipitation of Atenolol: The influence of the Organic Solvent and of the Processing Approach, *Journal of Supercritical Fluids*, Vol. 38, pp. 434-441, 2006.
- [2] Tenerio A., Gordillo M. D., Pereyra C. M. and Martinez de la Ossa E. J., Screening Design of Experiment Applied to Supercritical Antisolvent Precipitation of Amoxicillin, *Journal of Supercritical Fluids*, Vol. 44, pp. 230-237, 2008.
- [3] Adami R., Osseo L. S., Huopalahti R. and Reverchon E., Supercritical Antisolvent Micronization of PVA by Semi-Continuous and Batch Processing, *Journal of Supercritical Fluids*, Vol. 44, pp. 288-298, 2007.
- [4] Miguel F., Martin A., Gamse T. and Cocero M. J., Supercritical Antisolvent Precipitation of Lycopene: Effect of the Operating Parameters, *Journal of Supercritical Fluids*, Vol. 36, pp. 225-235, 2006.
- [5] Chen K., Zhang X., Pan J. and Yin W., Recrystallization of Andrographolide Using the Supercritical Fluid Antisolvent Process, *Journal of Crystal Growth*, Vol. 274, pp. 226-232, 2005.
- [6] Kalogiannis C. G., Pavlidou E. and Panayiotou C. G., Production of

- Amoxicillin Microparticles by Supercritical Antisolvent Precipitation, *Industrial and Engineering Chemistry Research*, Vol. 44, pp. 9339-9346, 2005.
- [7] Warwick B., Dehghani F. and Foster N. R., Synthesis, Purification, and Micronization of Pharmaceuticals Using the Gas Antisolvent Technique, *Industrial and Engineering Chemistry Research*, Vol. 39, pp. 4571-4579, 2000.
- [8] Mukhopadhyay M. and Dalvi S.V., Mass and Heat Transfer Analysis of SAS: Effect of Thermodynamic States and Flow Rate on Droplet Size, *Journal of Supercritical Fluids*, Vol. 30, pp. 333-348, 2004.
- [9] Gioannis B. D., Jestin P. and Subra P., Morphology and Growth Control of Griseofulvin Recrystallized by Compressed Carbon Dioxide as Antisolvent, *Journal of Crystal Growth*, Vol. 262, pp. 519-526, 2004.
- [10] Neogy S., Das S., Mahapatra S. K., Mandal N. and Roy S., Amelioratory Effect of *Andrographis Paniculata* Needs on Liver, Kidney, Heart, Lung and Spleen During Nicotine Induced Oxidative Stress, *Environmental Toxicology and Pharmacology*, Vol. 25, pp. 321-328, 2008.
- [11] Li J., Cheung H. Y., Zhang Z., Chan G. K. L. and Fong W. F., Andrographolide Induces Cell Cycle Arrest at G2/M Phase and Cell Death in HepG2 Cells Via Alteration of Reactive Oxygen Species, *European Journal of Pharmacology*, Vol. 568, pp. 31-44, 2007.
- [12] Kumoro A. C. and Hasan M., Supercritical Carbon Dioxide Extraction of Andrographolide from *Andrographis Paniculata*: Effect of the Solvent Flow Rate, Pressure, and Temperature, *Chinese Journal of Chemical Engineering*, Vol. 15(6), pp. 877-883, 2007.
- [13] Constantinos G. K., Eleni P. and Constantinos G. P., Production of Amoxicillin Microparticles by Supercritical Antisolvent Precipitation, *Industrial and Engineering Chemistry Research*, Vol. 44, pp. 9339-9346, 2005.
- [14] Fages J., Lochard H., Letourneau J., Sauceau M. and Rodier E., Particle Generation for Pharmaceutical Applications Using Supercritical Fluid Technology, *Powder Technology*, Vol. 141, pp. 219-226, 2004.
- [15] Li G., Chu J., Song E. S., Row K. H., Lee K. H. and Lee Y. W., Crystallization of Acetaminophen Microparticle Using Supercritical Carbon Dioxide, *Korean Journal of Chemical Engineering*, Vol. 23(3), pp. 482-487, 2006.